Carbohydrate Polymers 83 (2011) 462–469

Contents lists available at ScienceDirect

Carbohydrate Polymers

journal homepage: www.elsevier.com/locate/carbpol

Design and investigation of nanoemulsified carrier based on amphiphile-modified hyaluronic acid

Ming Kong[a], Xiguang Chen[b], Hyunjin Park[a,*]

[a] Graduate School Biotechnology, Korea University, 1,5-Ka, Anam-Dong, Sungbuk-Ku, Seoul 136-701, South Korea
[b] College of Marine Life Science, Ocean University of China, Yushan Road, Shandong Province 266003, China

ARTICLE INFO

Article history:
Received 29 January 2010
Received in revised form 12 July 2010
Accepted 3 August 2010
Available online 11 August 2010

Keywords:
Hyaluronic acid
Monostearin
Nanoemulsion
Solvent evaporation
Methylene chloride

ABSTRACT

Hyaluronic acid (HA) was modified into an amphiphile through esterification between the carboxyl and hydroxyl moieties on glycerol-α-monostearate (GMS). The conjugation was verified via FT/IR and ^{1}H NMR. Ultrasonification and solvent evaporation were used to prepare a fine oil/water/surfactant (O/W/S) nanoemulsion consisting of methylene chloride as the oil phase (O), HA water solution (W), and non-ionic Tween-80 and Span-20 as surfactant (S). The optimal ratio of the disperse phase was screened in nanoemulsion formed without HA-GMS. Tween-80 and Span-20 at the required hydrophilic–lipophilic balance (HLB) of 12.5 and a ratio of O/S (ROS) of 60, which accounted for 5% (w/w) in the emulsion system, was determined to be the optimal disperse phase ratio, giving rise to the smallest droplet size (39.7 nm) and lower protein dispersibility (0.341). The smallest droplet size of the HA-GMS nanoemulsion was 42.0 nm, with contraction to 38.9 nm evident after 96 h storage. Higher degree of substitution or lower molecular weight was favorable for the formation of smaller emulsified droplets. Nanoemulsions were characterized morphologically by electronic microscopy.

1. Introduction

In the past few decades, intensive research interest has been directed at the use of lipid-based carriers (liposomes, single or multiple emulsions in either nanoscale or microscale) for topical applications, (Souto & Müller, 2008). By virtue of their fine droplet diameter, larger surface area to volume ratio, and novel physicochemical properties like thermodynamical variability and transparent appearance, nanoproducts such as nanocarriers have been especially studied (Bang, Yu, Hwang, & Park, 2009; Liu & Park, 2009; Sonneville-Aubrun, Simonnet, & L'Alloret, 2004; Xia, Li, & Nel, 2009). Although nanocarriers are lipid-based, their bioavailability is imparted by biopolymers encapsulated inside or coated on the exterior surface, or on the structure of the interior network. Typically, these biopolymers are of natural origin, and their biocompatibility and biodegradative characteristics are a function of their functional groups (i.e., chitosan, cellulose, hyaluronic acid, silicate, and alginate, etc.).

Hyaluronan (hyaluronic acid, HA) is one such naturally occurring polymer. HA is composed of unbranched repeating units of glucuronic acid and N-acetyl glucosamine linked by β1-3 and β1-4 glycosidic bonds (Ambrosio, Borzacchiello, Netti, & Nicolais, 1999). Properties of HA including specific viscoelasticity, biocompatibility, hydration and lubrication (Garg & Hales, 2004) make this polysaccharide potentially very useful in the food, medical and cosmetic industries. The presence of a carboxyl group on glucuronic acid C-5 makes HA an ideal substrate for covalent conjugation with amide and hydroxyl groups through amidification and esterification, respectively (Bencherif et al., 2008; Choi et al., 2008). The corresponding modified HA can be utilized in various forms including films, hydrogels, as scaffolding, and in nanoparticles (Bencherif et al., 2008; Choi et al., 2008; Hu, Wu, Cai, Ma, & Wang, 2009; Ren, Zhou, Liu, Xu, & Cui, 2009). Besides retaining their inherently superior properties, HA derivatives acquire additional physicochemical characteristics that can be tailored according to the desired requirements. So far, the application of HA derivatives has been mainly focused on pharmaceuticals, tissue engineering, and drug delivery. In contrast, cosmetic and food applications have received scant attention. A nanocarrier would represent a universal transporting medium and, hence, warrants more intensive study.

Amphiphilic modifications on molecules are a prerequisite for HA considering both its inherent structure and corresponding nanocarrier formulation. Amphiphilic HA can be synthesized through hydrophobic derivation on carboxyl or hydroxyl groups. The grafted hydrophobic portion can be provided by alkyl, amine, and poly-organic acid components (Choi et al., 2008; Lee, Ahn, & Park, 2009; Mlčochová et al., 2007). Noticeably, taking account of bioavailability, the introduced components should

* Corresponding author.
E-mail address: hjpark@korea.ac.kr (H. Park).

0144-8617/$ – see front matter © 2010 Elsevier Ltd. All rights reserved.
doi:10.1016/j.carbpol.2010.08.001

be nontoxic and nonirritating, thus, components that are biocompatible and natural occurring are preferred. In this study, glycerol α-monostearate (GMS), a saturated lipid whose precursor (stearic acid) occurs in many animal and vegetable fats and oils (http://en.wikipedia.org/wiki/Stearic_acid), acted as the counterpart. Amphiphiles enable formation of nanocarriers via self-assembly with energy input, with the hydrophobic regions directed inwards or outwards on the nanocarrier surface. Due to hampered capability in delivering a water-soluble active component, lipid-based carriers have become broadly utilized (Wang, Dong, Chen, Eastoe, & Li, 2009). Among these, nanoemulsions can be a substitute for less stable liposomes and vesicles (Tadros, Izquierdo, Esquena, & Solans, 2004).

Typically, nanoemulsions can be prepared by a continuous/dispersion phase system consisting of two immiscible phases. One example is the self-nanoemulsifying drug delivery system (SNEDDS), in which isotropic mixtures of oil, surfactants and cosurfactants form fine oil-in-water nanoemulsions upon mild agitation (Nazzal, Smalyukh, Lavrentovich, & Khan, 2002). Nanoemulsions are very fine emulsions with a droplet diameter basically smaller than 100 nm (range 50–200 nm) (Sonneville-Aubrun et al., 2004; Tadros et al., 2004). Fine size contributes to weak flocculation, coalescence, translucence and transdermal permeation, in which droplet size plays an important role, where smaller size allows for better performance (Shakeel et al., 2007).

In this article, we report on the synthesis of a new amphiphile through esterification between HA carboxyl groups and GMS hydroxyl groups, via crosslinking by 1-ethyl-3-(3-dimethylaminopropyl)-carbodiimide hydrochloride (EDC). The amphiphiles were then used to prepare a nanoemulsion in an oil/water/surfactant (O/W/S) emulsifying system, where water-solubilized HA-GMS acted as the continuous phase and methylene chloride as the oil phase. Our objective was to develop a new, smaller-sized HA nanocarrier in a way that is mild and safe, and which could be applicable to food, medical or cosmetic use.

2. Materials and methods

2.1. Materials

Sodium forms of HA with a molecular weight (MW) of 110 kDa and 10 kDa were a gift of Kolon Life Science, Korea. EDC and monostearin (glycerol α-monostearate, GMS) were purchased from Tokyo Kasei Kogyo Co., Ltd (Japan). N-Hydroxy succinimide (NHS, 97%) was acquired from Aldrich Chemical. Methylene chloride was purchased from Duksan Pure Chemical (Korea). Phosphate buffered saline (pH 7.4) was purchased from Sigma–Aldrich. Various surfactants, polyoxyethylene sorbitan fatty acid esters (Tweens) and sorbitan fatty acid esters (Spans) were purchased from Samchun Pure Chemical (Korea). Water, used for synthesis and characterization was purified by distillation, deionized and subjected to reverse osmosis using a Milli-Q Plus apparatus (Millipore, USA). All the chemicals were analytical grade and were used as received.

2.2. Synthesis of amphiphilic HA-GMS

GMS was conjugated to HA by the formation of ester linkages through an EDC-mediated reaction. HA (190 mg) and EDC/NHS were dissolved in PBS (pH 7.4 and 4.75, respectively). EDC/NHS solution was mixed with HA solution and maintained for 2 h to achieve a 1:1:1 mole ratio to glucuronic acid residue of HA. The solution was then added to GMS (60–540 mg) acetone solution dropwise with magnetic stirring. The reaction mixture was left at room temperature for 24–48 h. The resultant mixture was centrifuged at 15,000 rpm, 4 °C in a Beckman Coulter Avanti J-E apparatus for 20 min/cycle until the obtained solution was not turbid. The apparent solution was extensively dialyzed using a Spectra/Por Membrane with a MW cut-off of 6000–8000 against an excess volume of water/acetone (1:1 v/v–3:1 v/v)and distilled water for 3 days, followed by lyophilization using a model FD5518 lyophilizer (Ilshin Lab., Korea) for 3 days.

2.3. Evaluation of HA-GMS characteristics

Structure of the cotton-like HA-GMS was evaluated by Fourier transform infrared spectroscopy (FT/IR) and ^{1}H nuclear magnetic resonance (NMR) spectroscopy. The IR spectrum of HA-GMS was recorded on an FT/IR-430 spectrometer (Jasco, Tokyo, Japan) at 20 °C as previously described (Chen, Lee, & Park, 2003). ^{1}H NMR spectra of samples were measured using a Varian Unity Plus-300 spectrometer at ambient temperature. The sample was dissolved in deuterium oxide (D_2O) and measured using 4000 Hz width, 45° pulse angle, 3.744 s acquisition time, and 48 scans with a delay of 2 s between each scan. ^{1}H NMR spectroscopy was used to determine the esterification conversion on modified HA. Degree of substitution (DS) was defined as the amount of GMS groups per one HA disaccharide repeat unit, and was calculated from the ratio of the relative peak integrations of the GMS ending methyl protons (peaks at around approximately 1.0 ppm) and methyl protons in HA acetamide (approximately 2.0 ppm) (Mlčochová et al., 2007).

2.4. Optimum screening and preparation of nanoemulsions

Considering the synthetic cost and experimental usage of HA-GMS, preparation of nanoemulsions was divided into two major segments. The first was screening for the optimum proportion of the disperse phase without HA-GMS in the O/W/S emulsifying system, where distilled water acted as the water phase in nanoemulsion. The second was preparation of HA-GMS nanoemulsion with an optimal proportion.

2.4.1. Screening for the optimum surfactant proportion

An emulsifier blend for an optimal oil-in-water emulsion was determined using the Atlas HLB method (Atlas HLB System, 1963). A series of Tween and Span non-ionic emulsifiers were screened to determine the required hydrophile–lipophile balance (HLB) value, chemical type and concentration of the disperse phase for the preparation of a stable, small droplet size and low polydispersity oil-in-water emulsion. In this aspect, Span-80 (S80) and Tween-80 (T80) were selected as the surfactant blend to determine the required HLB value (O/W/S of 5:90:5 (w/w)) within 8–15. The HLB values of the surfactant mixtures (HLB_{mix}) were calculated according to literature (Wang et al., 2009) who also applied Spans and Tweens to adjust $HLB_{mix,}$ using the following equation:

$$HLB_{mix} = f_A HLB_A + f_B HLB_B$$

where HLB_A, HLB_B are the HLB values, and f_A, f_B are the weight fractions of Tween and Span, respectively. Mean size of droplets and polydispersity were taken into account together for determining the required HLB value. Using this value, variation in chemical types of surfactants was assessed to find the desired surfactants combination (O/W/S = 5:90:5 (w/w)). The optimum amount of the disperse phase was studied in gradient concentrations: 1, 2, 5, 10, 15, 20, 25, 30 and 35% (w/w). Upon the optimum conditions acquired, the desirable O/S ratio, ranging from 0 to 100% (w/w) was then determined. The size distribution and phase separation observed during screening were considered as criteria for optimal choices. Preparation of nanoemulsions relied on sonication. The disperse phase composed of methylene chloride and surfactants were added dropwise into the distilled water continuous phase, and a coarse

emulsion formed after a 5 min period of magnetic stirring at 20 °C. The coarse emulsion was further sonicated with a Sonics Vibra-Cell CV33 ultrasonic probe (Sonics & Materials, USA) at 150 W in an ice bath for 3 min. The sonication step was repeated two times using a pulse function (pulse on, 10.0 s; pulse off, 2.0 s).

2.4.2. Preparation of HA-GMS nanoemulsion

Preparation of the HA-GMS nanoemulsion differed slightly from that for HA-GMS-free nanoemulsion. For the former, the disperse phase was added dropwise to a HA-GMS PBS solution (1 mg/mL) instead of distilled water for formation of the coarse emulsion. The coarse emulsion was further pulse-sonicated twice as described above. Different from HA-GMS-free nanoemulsion, based on practical and secure consideration, HA-GMS nanoemulsion was evaporated under reduced pressure for 30 min at room temperature to remove methylene chloride.

2.5. Measurement of nanoemulsion properties

2.5.1. Size and distribution analysis

The average particle size, polydispersity index (PdI) and zeta potential were determined by quasielastic laser light scattering using a Zetasizer ZEN 3600 Nano Series apparatus (ZEN, UK). PdI is a parameter used to define the particle size distribution of nanoparticles obtained from photon correlation spectroscopic analysis. It is a dimensionless number extrapolated from the autocorrelation function (Nidhin, Indumathy, Sreeram, & Nair, 2008). The calculation for PdI is defined in ISO standard document 13321:1996. Presently, aliquots of the nanoemulsions were put into polystyrene latex cells and measured at a detector angle of 90°, wavelength of 633 nm, refractive index of 1.33, real refractive index was 1.423 (methylene chloride) in HA-GMS-free nanoemulsion and was 1.46 (HA) in HA-GMS nanoemulsion, and temperature of 25 °C. Since the mean nanoemulsion droplet size varied over time during room temperature storage, the variations were traced across time from 0 to 96 h and size distributions were measured for different samples.

2.5.2. Confocal laser scanning microscopy (CLSM)

Since screening and preparation of HA-GMS nanoemulsions were conducted separately, evidence for existence of HA-GMS on the nanoemulsion surface was necessary. HA-GMS (10 kDa) was labeled with rhodamine (Lee, Mok, Lee, Oh, & Park, 2007) with minor modification. Briefly, HA-GMS PBS (pH 7.4) was mixed with EDC/HNS and left for 2 h. Rhodamine PBS (pH 7.4) was added and allowed to react for 2 h at 20 °C. The resulting solution was dialyzed against distilled water for 24 h and lyophilized. Nanoemulsion was prepared with the rhodamine-labeled HA-GMS. With the corresponding HA-GMS solution as a control, CLSM images were obtained using a LSM 5 Exciter apparatus (Carl-Zeiss, USA) at an excitation wavelength of 543 nm.

2.5.3. Transmission electron microscopy (TEM)

Specimens were prepared by dropping the sample solution onto a carbon-coated copper grid. The specimens were allowed to air-dry prior to TEM examination using Tecnai G2 F30 microscope (Philips-FEI, Holland). TEM studies were conducted at KBSI (Seoul).

2.6. Statistical analysis

The assays were performed at least in triplicate on separate occasions. The data collected in this study are expressed as the mean ± standard deviation.

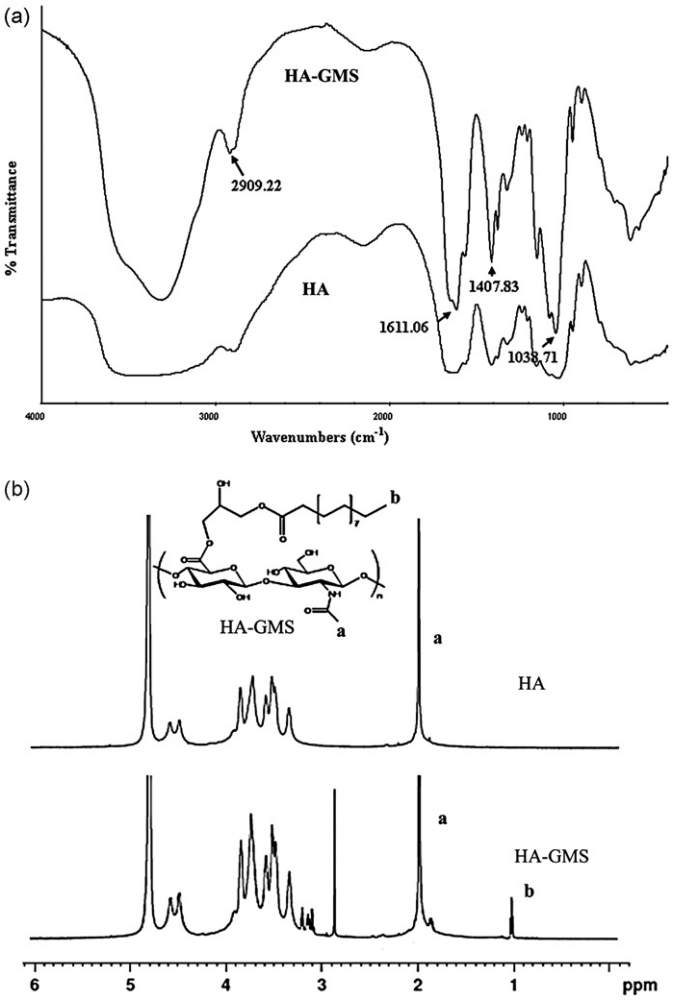

Fig. 1. (a) FT/IR spectra; (b) ^{1}H NMR of HA and HA-GMS.

3. Results and discussion

3.1. Synthesis and characterizations of HA-GMS

In the course of synthesis, different mole ratios of HA/GMS from 3:1 to 1:3, different pHs (4.75 and 7.4), and different synthesizing times (24 and 48 h) were used to attain different DS of HA-GMS with yields around 90%.

FTIR spectra of HA and HA-GMS are shown in Fig. 1a. The absorption bands at 3200–3600 cm^{-1} corresponded to the OH group of HA, 1850–1630 cm^{-1} and 1260–1000 cm^{-1} were attributed to the C=O and C–O bonds respectively, and stretching vibrations near 2900 cm^{-1} and 1400–1500 cm^{-1} were assigned for sp^3 and sp^2 C–H stretches. Since the introduction of carbohydrate chains via esterification, all of the absorptions above were sharper for HA-GMS than those for HA, which verified the linkage of GMS monomers onto HA chains.

The amount of crosslinked GMS on HA was quantitatively characterized from the ^{1}H NMR spectra using the integration method. The characteristic peaks of N-acetyl group of HA (δ/ppm = 2.0 [t, 3H, $-COCH_3$]) and GMS (δ/ppm 1.0 [t, 3H, $CH_3-(CH_2)_{16}-$]) were used for integration (Fig. 1b). As shown in Table 1, the DS of the different products varied from 6.16 to 23% for HA-GMS (110 kDa), with essentially no change for lower MW HA-GMS in all cases. The pH values were selected based on two observations: First, conjugation crosslinked by carboiimide is most efficiently performed at pH 3.5–4.5 (Nakajima & Ikada, 1995) and, since HA is unstable in

Table 1
DS of HA-GMS synthesized under different conditions.

Time (h)	$N_{HA:GMS}$ pH 7.4				$N_{HA:GMS}$ pH 4.75	
	1:3	1:1	2:1	3:1	1:3	1:1
HA (110 kDa)						
24	–	6.50%[a]	6.21%	6.16%	–	–
48	23%[b]	14%[c]	–	–	16%	7%
HA (10 kDa)						
48	6%	6%[d]	–	–	5%	5%

"–" denotes no detection.
Superscripts indicate different samples: [a]H6.5; [b]H14; [c]H23; [d]L6, where characters denoted MW property of HA and the latter numbers are DS of HA-GMS.

an acid solution, pH 4.75 was chosen. Secondly, pH 7.4 was used in the preparation of HA films using EDC as the crosslinking reagent (Young, Cheng, Tsou, Liu, & Wang, 2004). The DS of the products suggested that excess GMS and neutral pH condition promotes a higher DS value.

Upon consideration of the costs of synthesis and pH consistency, gradient DS samples were picked and labeled as H6.5, H14, H23 and L6 (Table 1), where the characters denote the MW property of HA and the numbers were the DS for specific samples.

3.2. Screening of optimal surfactant ration

3.2.1. Determination of required HLB

With our major study target being to prepare a stable and small droplet size nanocarrier, an emulsion was employed. In general, nanoemulsions as stable against sedimentation or creaming owing to their small droplet size (Forgiarini, Esquena, González, & Solans, 2001). However, they are metastable systems, whose structures depend on the preparative process (Sonneville-Aubrun et al., 2004). For whatever emulsion system, the choice of the correct emulsifier is very crucial to improvement of emulsion stability (Sajjadi, 2006). Certain mixtures of surfactants can provide better performance than use of a single surfactant (Rosen, 1992; Scamehorn, 1986). In a mixed non-ionic surfactant system, HLB has been proven to be very useful in attaining the best type of emulsifier for any given oil phase (Gullapalli & Sheth, 1999; Wang et al., 2009); the best type of emulsifier is designated the required HLB. For O/W emulsions, surfactants with higher HLB tend to stabilize the system, thus, HLB values ranging from 8 to 15 were presently chosen, from which the required HLB was obtained.

From the correlation between HLB and mean droplet size (Fig. 2a), the curve of mean droplet size exhibited a declining trend rather than the spoon shape reported previously (Wang et al., 2009). This was probably attributable to the finite solubility of methylene chloride in water. Methylene chloride was chosen as the oil phase, based partly on its ability to diffuse into the aqueous phase at a rapid rate facilitating particle formation upon evaporation (Lemos-Senna, Wouessidjewe, Lesieur, & Duchêne, 1998), which minimizes toxicity. Another reason for the choice of methylene chloride is that it offers solvent for lipophilic active ingredient, nutrient or drug before being evaporated. Referring to HLB calculation, higher values indicate surfactants own higher hydrophilicity, which facilitates reducing curvature of interface for the oil that owns relatively high solubility, leading to smaller droplet size. This is the likely explanation for the decreasing trend in mean droplet size. In this case, PdI was assessed simultaneously to determine the required HLB. Considering our primary aim of achieving smaller droplet size, HLB displaying a lower PdI, including 12, 12.5 and 13, met the demand (Fig. 2a). However, phase observation of nanoemulsions revealed that phase separation was inclined to occur for HLB 13 after 24 h, which rendered these nanoemulsions unstable in storage. Based on comprehensive consideration, 12.5 was selected as the required HLB for further study.

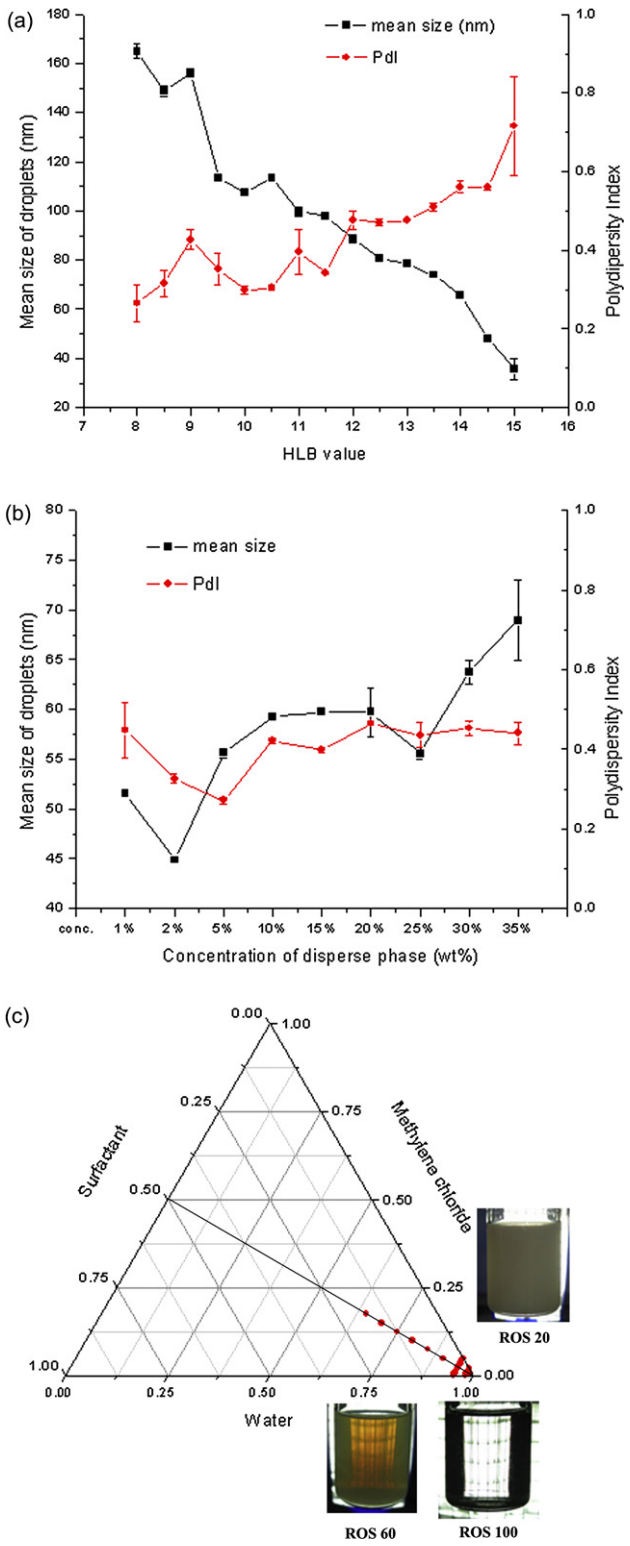

Fig. 2. Droplet size and polydispersity index of HA-GMS-free nanoemulsions, (a) as a function of surfactant HLB in O/W/S (5/90/5) system; (b) as functions of disperse phase concentration; (c) pseudo ternary diagram and emulsion appearances.

3.2.2. Optimal surfactants composition

At the required HLB, the optimum composition of the mixture of surfactants was screened using various pairs of emulsifiers.

Table 2
Correlation between size, PdI of HA-GMS free nanoemulsion, and compositions of surfactants mixture (O/W/S = 5:90:5, w/w).

Composition	Mean size (nm)	PdI
T20–S20	106.20 ± 0.20	0.399 ± 0.008
T20–S60	75.64 ± 1.48	0.607 ± 0.007
T20–S80	69.92 ± 0.19	0.579 ± 0.008
T60–S20	70.80 ± 0.32	0.322 ± 0.002
T60–S60	93.34 ± 0.45	0.519 ± 0.005
T60–S80	70.95 ± 0.18	0.399 ± 0.007
T80–S20	57.98 ± 0.25	0.418 ± 0.006
T80–S60	66.33 ± 0.52	0.570 ± 0.004
T80–S80	74.37 ± 0.81	0.480 ± 0.003

Note: T: Tween; S: Span.

As shown in Table 2, nanoemulsions with the smallest droplet size (58.0 nm) were prepared from the T80–S20 surfactant pair, which was composed of long chain hydrophilic (T80) and short chain lipophilic (S20) surfactants. Even at required HLB, in every three surfactants pairs consisting of the same Tween ingredient the smallest droplet sizes were obtained from the pairs with the largest differences in surfactants chain length (i.e. T60–S20, T20–S80 and T80–S20). In addition, pairs involving T80 (i.e., C18 unsaturated carbohydrate chain) displayed the smallest droplets size, consistent with previous observations (Wang et al., 2009). The collective results support the suggestion that variation in carbohydrate chain length between the Tween and Span, as well as the presence of a double bond in the chain, drive the formation of a looser film at the water/oil interface, which favors the formation of nanoemulsions with smaller droplet sizes.

3.2.3. Optimal ratio of surfactant of disperse phase

In addition to the required HLB and surfactant composition, the ratio of surfactant (ROS, defined as the weight percentage of surfactants in the disperse phase) is also indispensable in screening for optimal surfactants. Presently, prior to ROS measurement, gradient concentrations (0–35% wt%)of the disperse phase made up of T80–S20 and methylene chloride in equal proportions were emulsified in distilled water (Fig. 2b). With increasing concentration, the mean size of droplets initially reduced, being smallest at a concentration of 5%, and then increased slowly. A similar trend was evident for PdI, with the smallest droplet size occurring at a concentration of 2%. It was indicated that larger amount of disperse phase resulted in wider size distribution and larger droplet size. The smallest size did not come out with the lowest PdI, nevertheless, 5% concentration also gave rise to a relative smaller droplet size (55.6 nm). Furthermore, the 2% disperse phase concentration including surfactant (1% oil phase) for nanocarriers was apparently a small fraction for active component. Considering a practical application, a concentration of 5% was selected for the following ROS measurements.

ROS measurement was carried out in different ratios shown in Table 3. A ROS of 0, in which the disperse phase was comprised purely of methylene chloride, produced unstable nanodroplets on the basis of statistical analyses and by the visually apparent aggregation observed only moments after preparation. In the presence of surfactants, nanodroplet quality was obviously improved, exhibited a reduced mean size and lower PdI. At ROSs <70, incremental changes in the surfactant fraction led to decreasing droplet size and narrow size distribution. The smallest size appeared at ROS 60 (39.7 nm). With the exception of ROS 100, after ROS reached 70 size distribution in terms of PdI increased, which was likely attributable to the disproportion of excess surfactants and oil, which were unable to maintain the kinetic stability of the nanodroplets. Yet, pure surfactants could disperse well in the continuous phase. In an emulsion system, the oil phase requires a certain amount of surfactants to satisfy the demand for the formation of stable

Table 3
Size distribution of HA-GMS free nanoemulsion with various ROS (5% disperse phase).

ROS[a]	Mean size (nm)	PdI
0	264.03 ± 37.10	0.458 ± 0.059
10	112.23 ± 0.84	0.192 ± 0.008
20	98.04 ± 0.33	0.223 ± 0.002
30	82.70 ± 0.44	0.269 ± 0.009
40	66.80 ± 0.36	0.274 ± 0.004
50	49.31 ± 0.88	0.368 ± 0.012
60	39.74 ± 0.23	0.341 ± 0.007
70	40.65 ± 0.27	0.456 ± 0.008
80	37.93 ± 0.53	0.567 ± 0.023
90	123.63 ± 7.68	0.204 ± 0.010
100	48.23 ± 0.29	0.307 ± 0.006

[a] Ratio of wt% surfactants in disperse phase.

nanoemulsions. In the presence of excess surfactant, the surplus surfactants might themselves become emulsified as smaller size droplets, producing an increased PdI. If so, the reason(s) were not presently determined.

Fig. 2c depicts a pseudo ternary diagram of this emulsion and the appearances of the nanoemulsions in the corresponding ROS. The nanoemulsion was turbid when the oil fraction exceeded 50% (ROS = 20). With increasing surfactants (ROS = 60), the nanoemulsion became transparent, and was especially evident at ROS = 100. The different appearances and mean size of droplets reflected the smaller size leading to higher clarity. The results indicated that ROS 60 was the preferred ROS for our aim. Screening for optimal proportion of the disperse phase was conducted in HA-GMS-free nanoemulsions. In the case of HA-GMS nanoemulsions, ROS 50 and 60 were selected for subsequent study.

3.3. Characterization of HA-GMS nanoemulsions

In the course of the preparation of HA-GMS nanoemulsions, methylene chloride was used as oil phase, T80–S20 mixture as surfactant with ROS = 50 and 60, and different samples of HA-GMS (H6.5, H14, H23, and L6 solutions; each 1 mg/mL) as continuous phase accounted for 95% (w/w) in the emulsion system. Consistent with their amphiphilic nature, HA-GMS self-assembled on the surface of nanodroplets with methylene chloride as hydrophobic template, anchored by GMS. Rhodamine labeling of HA-GMS enabled labeled nanoemulsified droplets to emit red fluorescence when excited by a laser beam. The subsequent CLSM observations offered direct evidence for the existence of HA-GMS (sample L6) on the droplet surface (Fig. 3). For emulsified groups, in which aggregation of labeled rhodamine occurred, nanodroplets were apparent based on brighter emitted fluorescence. In contrast, no fluorescence was found for the L6 solution control, due to rhodamine dissolution in solution. Furthermore, CLSM observations indicated an irregularly spherical droplet morphology.

3.3.1. Droplet size analysis

Mean size and size distribution were determined as soon as nanoemulsions were prepared. Variations of size were tracked at certain times up to 96 h (Fig. 4). For ROS 50 (Fig. 4a), all the samples displayed a decreasing trend in mean droplet size with time, from 58.4, 57.5, 56.4, and 51.3 nm in for H6.5, H14, H23, and L6, respectively, immediately following preparation, to 51.1, 49.9, 51.0, and 45.8 nm (same respective order) 96 h later. The variations were large during the first 24 h, but became smaller thereafter; a slight and transient rise was evident for L6. Similar trends were observed for ROS 60 (Fig. 4b), which varied from 54.8, 53.6, 51.2, 42.0 nm to 47.6, 43.8, 44.4, 36.9 nm (same respective order and time) for each sample, except for earlier appearance of a turning point at 12 h. Whatever the ROS, droplet size appeared to be invariable 72 h

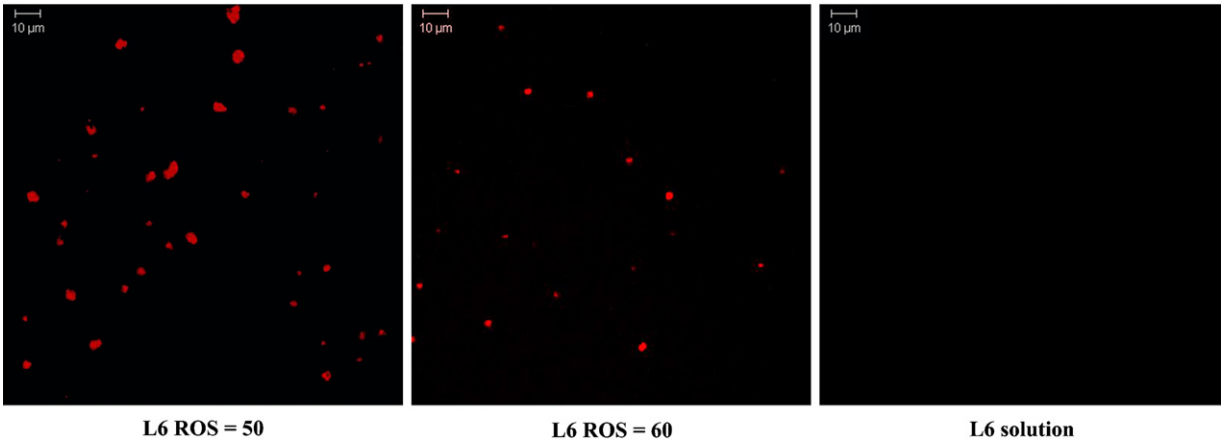

Fig. 3. CLSM of HA-GMS nanoemulsion (1 mg/mL) in methylene chloride/water/T80–S20 system. L6 solution was used as the control. ROS: ratio of wt% surfactants in the disperse phase. L6 indicates low MW HA-GMS with DS = 6%.

after preparation. Reduction of droplet size was mainly attributed to the evaporation of methylene chloride. Removal of the oil phase induced loss of the supporting template and led to contraction of these temporarily hollow particles. Since we did not utilize any crosslinking agent in this system, this contraction might have bestowed an unstable impact to the nanodroplets. During storage of nanoemulsions, instability was certainly observed; minor flocculation formed and precipitates were evident in emulsions. The instable phenomena probably arose from the soft nature of colloidal surfaces which made surfaces susceptible to collision and resulted in adherence between droplets, especially as rearrangement of surface components occurred in the course of size reduction. Zeta potential provided another evidence for instability, which ranged from −13.6 to −14.9 mV, and which was evidence of the unstable scope for nanoemulsions.

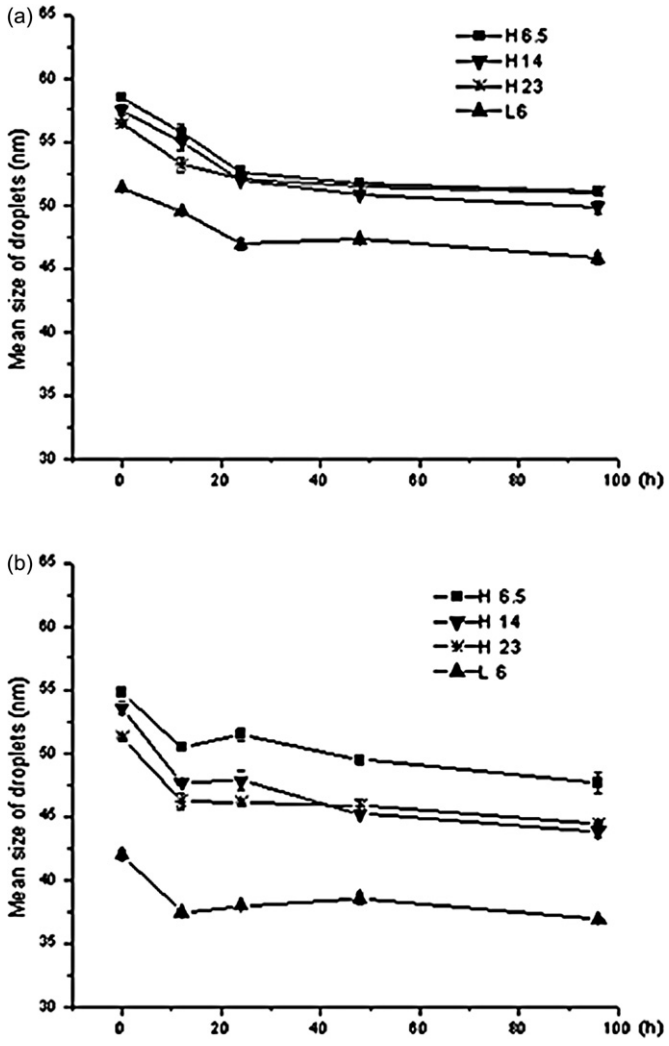

Fig. 4. Droplet size of HA-GMS nanoemulsions (1 mg/mL) in methylene chloride/water/T80–S20 system as a function of storage time. (a) ROS = 50; (b) ROS = 60. *Note*. ROS: ratio of wt% surfactants in disperse phase. H6.5 indicates high MW HA-GMS with DS = 6.5%; L6 indicates low MW HA-GMS with DS = 6%.

Regarding the MW of HA, nanoemulsions obtained from lower MW HA displayed an apparently smaller size in both ROS, which is entirely consistent given the relationship between nanoparticle size and material MW in which particle size decreases with decreasing MW (Janes & Alonso, 2003). The reason may be a MW-mediated molecular architecture. Presently, low MW HA owns small extent of polymerization and gives rise to short carbohydrate chains and small molecular size, which render high chain flexibility to assemble, small three-dimensional structures and weak steric interference, favoring the formation of a compact assembly of HA-GMS on the surface of droplets. Comparatively, bulky properties and strong steric hindrance of high MW HA give a larger droplet size. With respect to the effect of DS of HA, higher DS samples with the same MW showed a smaller size that was independent of ROS (i.e., H23 showed the smallest size in the first 24 h for ROS 50). However, the differences were not apparent at 96 h. Likewise, for ROS 60, higher DS samples consistently maintained a superior smaller size. The smallest size observed was 36.9 nm for L6 at 96 h. The result agrees with a report that higher DS produces smaller O-CMC nanoparticles (He & Zhao, 2007). The explanation is likely a more compact structure of HA-GMS layer caused by the larger amount of hydrophobic groups in higher DS samples, leading to stronger hydrophobic effects which enhance their adsorption on to the oil droplets and boost compactness of HA-GMS layer through chain–chain interactions. The complex effects decrease particle size consequently. The results support the suggestion that lower MW of HA or higher DS of HA-GMS drives the formation of smaller sized particles.

Besides the similarities from both ROS, some differences appeared, among which the significant one referred to droplet size. As discussed above, HA-GMS free nanoemulsions formulated with ROS 50 and 60 in distilled water varied in droplet size (Table 3). The features ought to be remained in a HA-GMS emulsion system (Fig. 4). Table 4 offers a direct and concise comparison. A noteworthy aspect of Table 4 is the control groups, despite equivalent nanoemulsion formation in distilled water, the mean droplet sizes

Table 4
Overall trend in mean size of HA-GMS nanoemulsions (1 mg/mL) in methylene chloride/water/T80–S20 system for each detected ROS over time.

ROS[a]	Mean size of droplets (nm)					
	Control	0 h	12 h	24 h	48 h	96 h
50	37.04 ± 0.07	56.16 ± 2.96	53.57 ± 2.59	50.89 ± 2.34	50.55 ± 2.13	49.42 ± 2.27
60	31.18 ± 0.34	50.37 ± 2.26	45.43 ± 5.08	45.82 ± 4.98	44.77 ± 4.13	43.19 ± 4.13

Note: Control is nanoemulsion without HA-GMS, formed by oil, surfactants, and distilled water.
[a] Ratio of wt% surfactants in disperse phase.

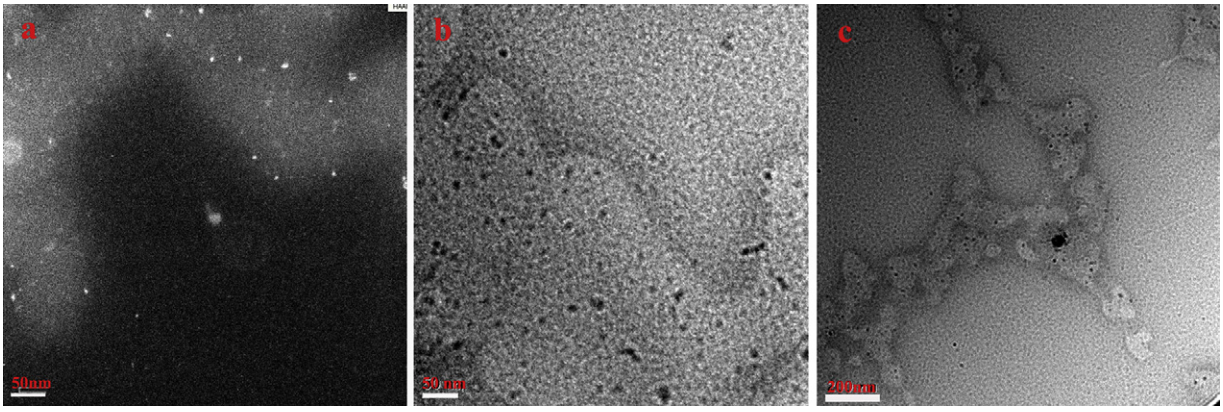

Fig. 5. TEM of HA-GMS nanoemulsion (1 mg/mL) in methylene chloride/water/T80–S20 system. (a) ROS = 50; (b) ROS = 60; (c) flocculation in ROS = 50. ROS: ratio of wt% surfactants in disperse phase.

differ from those in Table 3. All the nanoemulsion preparations in this table involved vacuum evaporation to eliminate methylene chloride, which would stimulate contraction of droplets. Comparison of nanoemulsions with and without HA-GMS clearly shows that the presence of HA-GMS increases the average size of particles in the manner of layer formulation on droplets' surface. As anticipated, on overall view, ROS 60 showed an average smaller size based on all the samples in comparison with ROS 50.

3.3.2. TEM

TEM was carried out after desiccation. ROS 50 and 60 with H23 were taken as observational samples (Fig. 5a and b). The blurry shadows on the background in each figure were due to retention of stain by water. It was shown that the nanodroplets were spherical and the average sizes (approximately 6 nm) were far smaller than the mean size measured by Zetasizer and the results observed in LCSM (Fig. 3). ROS 60 produced more consistently sized particles than ROS 50. The substantial reduction in droplets size, for one hand, arose from the dry process, which gave rise to size contraction. For another, remove of template, methylene chloride, the mass loss rendered relocation of surfactants and HA-GMS in body of spherical particles. Thirdly, the sizes measured by Zetasizer are hydrodynamic sizes, which featured by combination of water molecules on the HA chains and which likely enlarge particle size. Besides the emulsion samples, flocculation that formed on the bottom of nanoemulsion was sampled for TEM. A network of filaments was observed in the flocculation on a 1 μm scale. As shown in Fig. 5c, at a higher magnification, the fileceous structures were composed of particles and inter-matrix, nevertheless, aggregation of particles was not found. These phenomena reflect the instability of the nanoemulsion.

4. Conclusions

In this study, a new HA based nanoemulsion with average size smaller than 100 nm was introduced. HA amphiphile was synthesized in a mild and secure fashion through esterification. Serial of HA-GMS with different DS and Mw were obtained by modulating HA Mw and molar ratio of HA and GMS. HA-GMS nanoemulsion was prepared using O/W/S emulsion via ultrasonication, where methylene chloride as oil phase, HA-GMS water solution as continuous phase, mixture of Tween and Span as surfactant. Solvent evaporation involved in formation of HA-GMS nanoemulsion to remove oil phase. The optimal ratio of disperse phase occupied 5% (w/w) in emulsion system, composing of Tween 80 and Span 20 at required HLB 12.5 accounting for 60%. Mean size of HA-GMS nanoemulsion appeared to be bigger than HA-GMS free nanoemulsion. Higher DS or lower Mw was favored to form smaller emulsified droplets. LCSM and TEM observations proved the particles in nanoemulsion were spherical and evenly distributed. HA's advantageous bioavailability and the smaller size of the produced nanoemulsion certainly enable it to be a potential nanocarrier either for lipophilic active ingredient, nutrients, or drugs, and exert promising and unique efficacies compared with the large size carriers.

Acknowledgment

This study was supported by a Grant of the Korea Health 21 R&D Project, Ministry of Health and Welfare, Republic of Korea (A050376).

References

Ambrosio, L., Borzacchiello, A., Netti, P. A., & Nicolais, L. (1999). Rheological study on hyaluronic acid and its derivative solutions. *Journal of Macromolecular Science, Part A, 36*, 991–1000.
Atlas HLB System. (1963). *A time-saving guide to emulsifier selection* (third ed.). Wilmington: Atlas Chemical Industries., pp. 7–13
Bang, S. H., Yu, Y. M., Hwang, I. C., & Park, H. J. (2009). Formation of size-controlled nano carrier systems by self-assembly. *Journal of Microencapsulation, 26*, 722–733.
Bencherif, S. A., Srinivasan, A., Horkay, F., Hollinger, J. O., Matyjaszewski, K., & Washburn, N. R. (2008). Influence of the degree of methacrylation on hyaluronic acid hydrogels properties. *Biomaterials, 29*, 1739–1749.
Chen, X. G., Lee, C. M., & Park, H. J. (2003). O/W emulsification for the self-aggregation and nanoparticle formation of linoleic acids modified chitosan in the aqueous system. *Journal of Agricultural and Food Chemistry, 5*, 3135–3139.

Choi, K. Y., Lee, S., Park, K., Kim, K., Park, J. H., Kwon, I. C., et al. (2008). Preparation and characterization of hyaluronic acid-based hydrogel nanoparticles. *Journal of Physics and Chemistry of Solids*, *69*, 1591–1595.

Forgiarini, A., Esquena, J., González, C., & Solans, C. (2001). Formation and stability of nanoemulsion in mixed nonionic surfactant systems. *Progress in Colloid and Polymer Science*, *118*, 184–189.

Garg, H. G., & Hales, C. A. (2004). *Chemistry and biology of hyaluronan*. London: Elsevier Science & Technology Books.

Gullapalli, R. P., & Sheth, B. B. (1999). Influence of an optimized non-ionic emulsifier blend on properties of oil-in-water emulsions. *European Journal of Pharmaceutics and Biopharmaceutics*, *48*, 233–238.

He, F., & Zhao, D. (2007). Manipulating the size and dispersibility of zerovalent iron nanoparticles by use of carboxymethyl cellulose stabilizers. *Environmental Science & Technology*, *41*, 6216–6221.

Hu, Y., Wu, Y., Cai, J., Ma, S., & Wang, X. (2009). The procoagulant properties of hyaluronic acid-collagen (I)/chitosan complex film. *Journal of Biomaterials Science, Polymer Edition*, *20*, 1111–1118.

Janes, K. A., & Alonso, M. J. (2003). Depolymerized chitosan nanoparticles for protein delivery: Preparation and characterization. *Journal of Applied Polymer Science*, *88*, 2769–2776.

Lee, H., Ahn, C. H., & Park, T. G. (2009). Poly[lactic-co-(glycolic acid)]-grafted hyaluronic acid copolymer micelle nanoparticles for target-specific delivery of doxorubicin. *Macromolecular Bioscience*, *9*, 336–342.

Lee, H. K., Mok, H. J., Lee, S. H., Oh, Y. K., & Park, T. G. (2007). Target-specific intracellular delivery of siRNA using degradable hyaluronic acid nanogels. *Journal of Controlled Release*, *119*, 245–252.

Lemos-Senna, E., Wouessidjewe, D., Lesieur, S., & Duchêne, D. (1998). Preparation of amphiphilic cyclodextrin nanospheres using the emulsification solvent evaporation method: Influence of the surfactants on preparation and hydrophobic drug loading. *International Journal of Pharmaceutics*, *170*, 119–128.

Liu, N., & Park, H. J. (2009). Chitosan-coated nanoliposome as vitamin E carrier. *Journal of Microencapsulation*, *26*, 235–242.

Mlčochová, P., Hájková, V., Steiner, B., Bystrický, S., Kóóš, M., Medová, M., et al. (2007). Preparation and characterization of biodegradable alkylether derivatives of hyaluronan. *Carbohydrate Polymers*, *69*, 344–352.

Nakajima, N., & Ikada, Y. (1995). Mechanism of amide formation by carbodiimide for bioconjugation in aqueous media. *Bioconjugate Chemistry*, *6*, 123–130.

Nazzal, S., Smalyukh, I. I., Lavrentovich, O. D., & Khan, M. A. (2002). Preparation and in vitro characterization of a eutectic based semisolid self-nanoemulsified drug delivery system (SNEDDS) of ubiquinone: Mechanism and progress of emulsion formation. *International Journal of Pharmaceutics*, *235*, 247–265.

Nidhin, M., Indumathy, R., Sreeram, K. J., & Nair, B. U. (2008). Synthesis of iron oxide nanoparticles of narrow size distribution on polysaccharide templates. *Bulletin of Materials Science*, *31*, 93–96.

Ren, Y. J., Zhou, Z. Y., Liu, B. F., Xu, Q. Y., & Cui, F. Z. (2009). Preparation and characterization of fibroin/hyaluronic acid composite scaffold. *International Journal of Biological Macromolecules*, *44*, 372–378.

Rosen, M. J. (1992). *In mixed surfactant systems*. Washington: American Chemical Society.

Sajjadi, S. (2006). Effect of mixing protocol on formation of fine emulsions. *Chemical Engineering Science*, *61*, 3009–3017.

Scamehorn, J. F. (1986). *Phenomena in mixed surfactant systems*. Washington: American Chemical Society.

Shakeel, F., Baboota, S., Ahuja, A., Ali, J., Aqil, M., & Shafiq, S. (2007). Nanoemulsions as vehicles for transdermal delivery of aceclofenac. *AAPS PharmSciTech*, *8*, 191–199.

Sonneville-Aubrun, O., Simonnet, J.-T., & L'Alloret, F. (2004). Nanoemulsions: A new vehicle for skincare products. *Advances in Colloid and Interface Science*, *108–109*, 145–149.

Souto, E. B., & Müller, R. H. (2008). Cosmetic features and applications of lipid nanoparticles (SLN, NLC). *International Journal of Cosmetic Science*, *30*, 157–165.

Tadros, T., Izquierdo, P., Esquena, J., & Solans, C. (2004). Formation and stability of nanoemulsions. *Advances in Colloid and Interface Science*, *108–109*(20), 303–318.

Wang, L., Dong, J., Chen, J., Eastoe, J., & Li, X. (2009). Design and optimization of a new self-nanoemulsifying drug delivery system. *Journal of Colloid and Interface Science*, *330*, 443–448.

Xia, T., Li, N., & Nel, A. E. (2009). Potential health impact of nanoparticles. *Annual Review of Public Health*, *30*, 137–150.

Young, J. J., Cheng, K. M., Tsou, T. L., Liu, H. W., & Wang, H. J. (2004). Preparation of cross-linked hyaluronic acid film using 2-chloro-1-methylpyridinium iodide or water-soluble 1-ethyl-(3,3-dimethylaminopropyl) carbodiimide. *Journal of Biomaterials Science, Polymer Edition*, *15*, 767–780.